galaxies

MDPI

Article

Relic—Shock Connection in Abell 115

Andrea Botteon [1,2,*], Fabio Gastaldello [3], Gianfranco Brunetti [2] and Daniele Dallacasa [1,2]

[1] Dipartimento di Fisica e Astronomia, Università di Bologna, via C. Ranzani 1, I-40127 Bologna, Italy; ddallaca@ira.inaf.it

[2] INAF - Istituto di Radioastronomia, via P. Gobetti 101, I-40129 Bologna, Italy; brunetti@ira.inaf.it

[3] INAF - Istituto di Astrofisica Spaziale e Fisica Cosmica, via E. Bassini 15, I-20133 Milano, Italy; gasta@iasf-milano.inaf.it

* Correspondence: botteon@ira.inaf.it

Academic Editors: Stefano Ettori and Dominique Eckert

Received: 9 September 2016; Accepted: 15 November 2016; Published: 23 November 2016

Abstract: Giant radio relics are arc-shaped diffuse sources with Mpc-scale found in the peripheries of some dynamically disturbed galaxy clusters. According to the leading scenario of relic formation, shock waves occurring in merger events amplify the local magnetic field and (re)accelerate particles. However, Mach numbers associated with merger shocks are typically low, and hence inefficient at accelerating particles from the thermal pool. We analyzed a deep *Chandra* observation (334 ks) to study the relic region in the cluster Abell 115. Temperature and surface brightness profiles taken across the relic both show a clear discontinuity, which is consistent with a shock. This result supports the relic–shock connection and represents a test case to study the origin of radio relics. In this particular case, we suggest that a re-acceleration scenario is more suitable. The relic morphology and position are consistent with a shock produced in an off-axis merger between clusters with different masses.

Keywords: shock waves; radiation mechanisms; non-thermal processes; galaxy clusters

1. Introduction

Galaxy clusters are the largest and most massive gravitationally bound systems in the Universe, reaching linear sizes of a few Mpc and masses up to 10^{15} $M_{\odot}$. Although the richest clusters may contain thousands of galaxies in their volume, galaxies account only for ∼5% of the cluster total mass which is instead dominated for about ∼80% by dark matter. The remaining ∼15% is in form of intra-cluster medium (ICM), a tenuous ($n_e \sim 10^{-3} - 10^{-4}$ cm^{-3}) and hot ($T \sim 10^7 - 10^8$ K) plasma whose thermal emission is detectable in the X-rays. In the past decades, radio observations detected also diffuse sources in some merging state systems, revealing the presence of magnetic fields and cosmic rays (CR) spread over the cluster volume, e.g., [1]. These Mpc-scale emissions are characterized by steep synchrotron spectra ($\alpha > 1$, with $S_\nu \propto \nu^{-\alpha}$) and can be divided in two classes. Radio halos are located in the cluster centers, appear with roundish morphologies, somewhat recalling the thermal ICM emission. Radio relics, instead, are typically found in cluster outskirts, have elongated shapes and strongly polarized, up to 60%–70% levels. Although their origin is still under debate, nowadays the most attracting scenario is that the turbulence induced during cluster merger (for halos) and the shocks (for relics) occurring in merger events are capable to (re)accelerate CRs and amplify magnetic fields allowing the synchrotron radiation over such large scales, e.g., [2].

We report a study of the relic region in Abell 115 (hereafter A115), a moderate redshift ($z = 0.197$) galaxy cluster very luminous in the X-rays ($L_{[0.1-2.4\,\mathrm{keV}]} = 1.5 \times 10^{45}$ erg s^{-1}) which is in a merging state. The combination of an archival *Very Large Array* (VLA) dataset and the new deep *Chandra* observations gives interesting insights about the relic origin. Calculations are performed by assuming a concordance ΛCDM cosmology with $H_0 = 70$ km s^{-1} Mpc^{-1}, $\Omega_m = 0.3$ and $\Omega_\Lambda = 0.7$, for which $1''$ corresponds to 3.261 kpc at the redshift of A115 ($z = 0.197$). All errors are quoted at 68%.

2. Observations

2.1. Chandra

We analyzed five ACIS-I *Chandra* observations of A115 (ObsID: 3233, 13458, 13459, 15578, 15581) in VFAINT mode. Soft proton flares detection and subtraction was performed by inspecting the light curves of chip S3 (for ObsID: 3233, 13459, 15581) and of a cluster free emission region in one ACIS-I chip (for ObsID: 13458, 15578) using the lc_filter routine. After this procedure, the resulting cleaned total exposure time was 334 ks. A 0.5–2 keV image of the cluster is reported in Figure 1a.

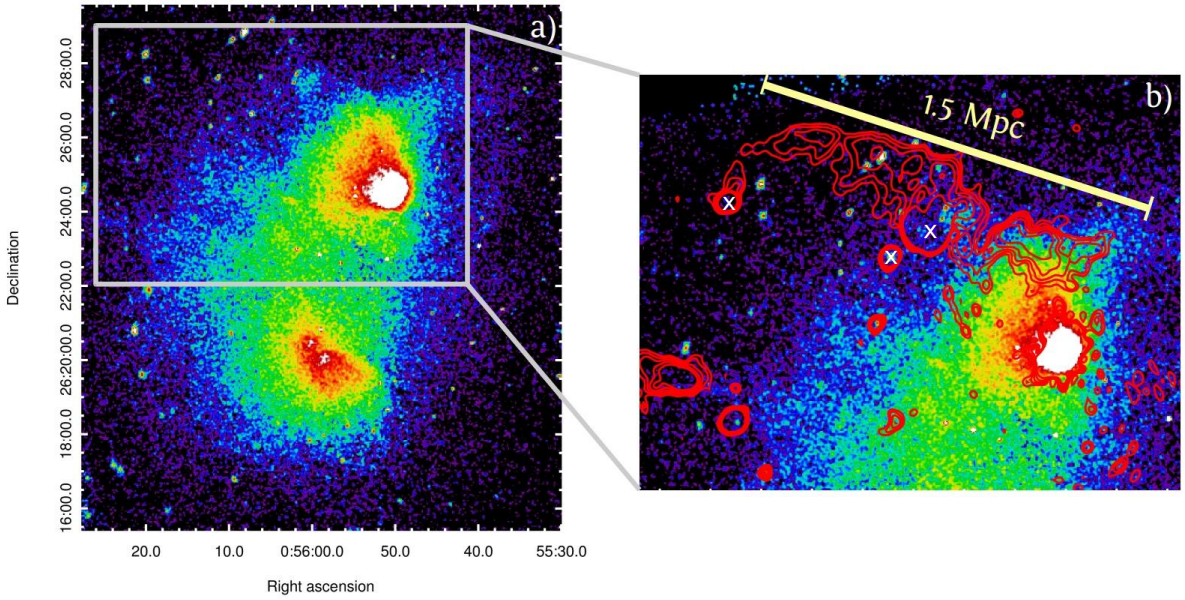

Figure 1. (**a**) *Chandra* view of A115 in the 0.5–2 keV band. The image is smoothed on a 3″ scale; (**b**) Zoom of the relic region. The Very Large Array (VLA) 1.4 GHz contours are shown in red, levels are $0.21 \times \pm(\sqrt{2})^n$ mJy b^{-1}, with $n = 1, 2, 3, 4$. The resolution is 15″ × 14″. The white crosses denote the radiogalaxies in the E relic region.

Surface brightness (SB) profile extraction and fitting was performed with PROFFIT v1.3 [3]. Discrete sources were detected using the wavdetect task on the merged image using a point spread function map with minimum size. Sources were visually confirmed and excluded in the further analysis. A background image was obtained by matching the background templates for every single ObsID and normalizing by counts in the 9.5–12 keV band. This was subtracted in the SB profile fits.

Spectral analysis was performed with XSPEC v12.9.0. Three background components were modeled in the fits: the Galactic background (taken into account with two thermal plasmas with temperatures 0.14 and 0.25 keV), the cosmic X-ray background (taken into account assuming an absorbed power-law with photon index 1.4) and the ACIS-I particle background (modelled following [4]). Since the low X-ray count rate, Cash statistics and an ICM metallicity fixed at 0.3 $Z_\odot$ were adopted in the fits.

2.2. VLA

We re-analyzed archival VLA observations of A115 at 1.4 GHz in C and D configurations (project code AF0349, see [5] for more details). Bad data due to radio frequency interference were excluded in the editing process, then the two datasets were phase-only self-calibrated independently a number of times. The data of IF1 (at 1364 MHz) for both datasets were combined after an accurate check on the sources flux densities. The total on-target observing time was 4.5 h and the bandwidth $\Delta\nu = 50$ MHz. After a number of self-calibration iterations, images were created adopting a two-scale clean procedure

in order to better recover the diffuse extended emission. The final image of the radio relic shown in Figure 1b has a restoring beam of $15'' \times 14''$ in position angle $-35°$. The 1σ off-source noise level is 70 μJy b^{-1}. A 5% uncertainty on the absolute flux scale calibration was assumed.

3. Relic–Shock Connection

3.1. Shock Detection

A115 is a galaxy cluster with a very irregular X-ray morphology which hosts a giant (∼1.5 Mpc) radio relic in its N periphery (Figure 1). Previous X-ray [6–8] and optical [9] studies of the cluster both concluded that A115 is undergoing an off-axis merger. The presence of a radio relic [5] is also an indication of the disturbed dynamical state of the system, as relics have been found only in unrelaxed systems [1,2]. In particular, an increasing number of relics is detected in coincidence of shock waves, e.g., [10–16], where particle (re)acceleration and magnetic field amplification occur.

By inspecting the X-ray image of A115 (Figure 1a), we noticed the presence of a SB drop in the cluster N region, where the W part of the relic stands out. For this reason we performed SB and spectral analysis in the sectors shown in Figure 2a. We fitted the SB profile assuming an underlying density broken power-law in the form

$$\begin{aligned} n_d(r) &= \mathcal{C} n_0 \left(\frac{r}{r_{sh}}\right)^{a_1}, \quad \text{if} \quad r \leq r_{sh} \\ n_u(r) &= n_0 \left(\frac{r}{r_{sh}}\right)^{a_2}, \quad \text{if} \quad r > r_{sh} \end{aligned} \tag{1}$$

where r is the distance from the (red) sector center, r_{sh} is the shock radius, n_0 is the density normalization, a_1 and a_2 are the power-law indices and $\mathcal{C} \equiv n_d/n_u$ is the shock compression factor. Subscripts d and u denote downstream and upstream quantities, respectively. The fit shown in Figure 2b is a good description of the data (χ^2/d.o.f. $= 67.6/54$) and leads to $\mathcal{C} = 2.0 \pm 0.1$. By using the Rankine-Hugoniot jump conditions for a monatomic gas

$$\mathcal{C} \equiv \frac{n_d}{n_u} = \frac{4\mathcal{M}_{\rm SB}^2}{\mathcal{M}_{\rm SB}^2 + 3}, \tag{2}$$

it corresponds to a Mach number $\mathcal{M}_{\rm SB} = 1.7 \pm 0.1$. We looked for systematics uncertainties due to the sector choice by varying its opening and position angle, the radial range where the fit is performed and the shock curvature radius. These tests led the Mach number to vary within the range 1.4–2.

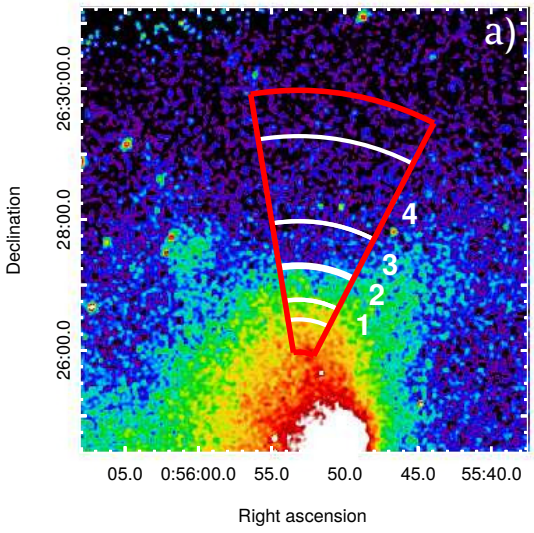

Figure 2. *Cont.*

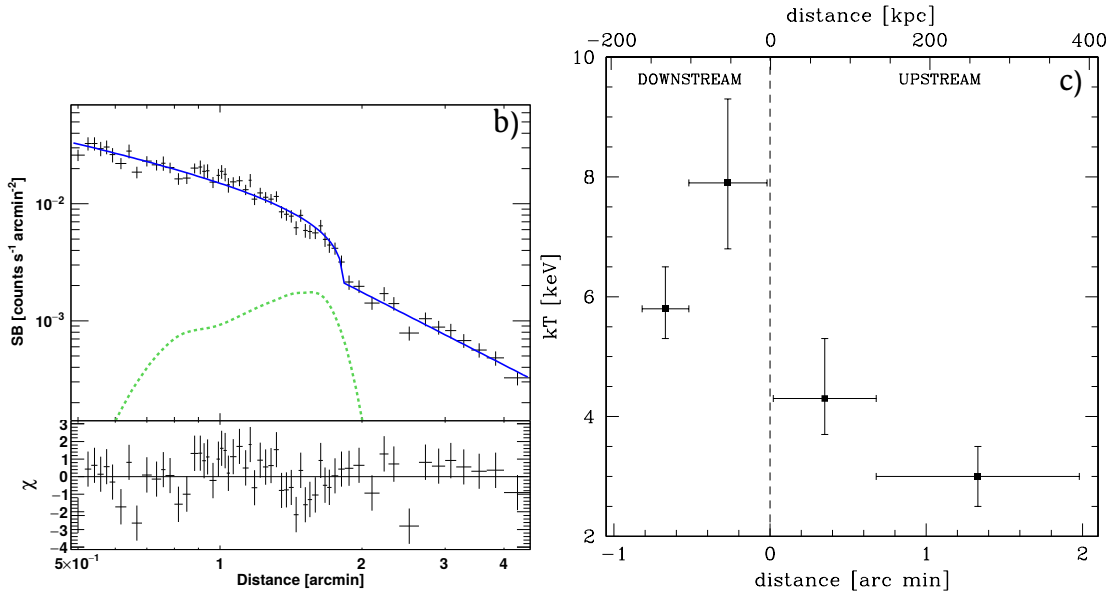

Figure 2. (**a**) Sectors used for the surface brightness (SB) (red) and spectral (white) analysis. The shock is between bin 2 and 3; (**b**) SB profile in the 0.5–2 keV band. The green dashed line shows the radio relic brightness profile (in arbitrary units); (**c**) Temperature profile across the shock. The vertical dashed line sets the location of the SB discontinuity.

In a shock wave, the downstream temperature is higher than the upstream one. For this reason, we performed spectral analysis in the relic region and produced the temperature profile shown in Figure 2c. In the two bins closer to the X-ray SB discontinuity, the temperature is $kT_d = 7.9^{+1.4}_{-1.1}$ keV and $kT_u = 4.3^{+1.0}_{-0.6}$ keV. This is consistent with the value expected from the SB drop since for a shock with $\mathcal{M} = 1.7$ the Rankine-Hugoniot conditions give $T_d/T_u \simeq 1.7$.

3.2. Relic Morphology and Location

The radio relic lays in the A115-N sub-cluster periphery and it is elongated in the E-W direction with a linear size ∼1.5 Mpc (Figure 1b). In the new 1.4 GHz VLA image at $15'' \times 14''$, the relic can be divided in two substructures defined by a "break" in its northern edge. The W part is short and straight and it coincides with the shock. This spatial connection supports the scenario in which particles are (re)accelerated in cluster shocks. The E part of the relic is instead arc-shaped, becoming thinner in the eastern direction. This region of the relic is harder to interpret as the low X-ray count statistics of this cluster region did not allow a proper investigation, hence it is not clear if it also traces a shock.

The position of the relic in A115 is not trivial to explain. In a head-on collision, outward moving shocks are expected to produce relics in opposite directions along the axis merger, e.g., [17]. However, both X-ray [8] and optical [9] studies on A115 concluded that the system is undergoing an off-axis merger, where the position of the shocks is complex to be determined and requires detailed numerical simulations. In particular, the location of the shock in A115 may be in agreement with the simulations of a merger with high impact parameter between clusters with unequal mass, where the shock curves around the core of the minor system (see Figure 7 in [18]), in agreement with A115-N sub-cluster being less massive [9]. This scenario could explain the unusual relic position and morphology: in particular, its E part would trace the uplifting of the cluster radiogalaxies (Figure 1b) plasma uplifted by the shock while it is moving in the outskirts.

3.3. Evidence of Particle Re-Acceleration?

There is broad consensus that shocks play a crucial role in powering radio relics in galaxy clusters. However, the diffuse shock acceleration (DSA) theory adopted to explain the CRs production in

Galactic supernova remnants (SNR) is severely challenged to reproduce the total radio luminosity of several relics, e.g., [2]. This problem is due to the typical low Mach numbers associated at cluster shocks ($\mathcal{M} \leq 3-4$) that would imply large acceleration efficiencies. Moreover, DSA from the thermal pool is further stressed by current γ-ray *Fermi* limits, assuming that the ratio of CR protons and electrons generated in cluster shocks is similar to that in SNRs, e.g., [19–21]. In this respect, re-acceleration models of a pre-existing population of CR electrons have been recently proposed, e.g., [22–25]. The detection of a shock co-spatially located with the radio relic in A115 thus provides an ideal test case to study particle (re)acceleration in cluster outskirts, since the properties of the underlying shock are well constrained.

The efficiency of electron acceleration η_e in a shock with speed V_{sh}, surface S and upstream mass-density ρ_u, is evaluated in order to reproduce the bolometric ($\geq \nu_0$) synchrotron luminosity

$$\int_{\nu_0} L(\nu)\, d\nu \simeq \frac{1}{2}\eta_e \Psi \rho_u V_{sh}^3 \left(1 - \frac{1}{\mathcal{C}^2}\right) \frac{B^2}{B_{cmb}^2 + B^2} S \tag{3}$$

where

$$\Psi = \frac{\int_{p_{min}} Q(p) E\, dp}{\int_{p_0} Q(p) E\, dp} \tag{4}$$

accounts for the ratio of the energy flux injected in "all" electrons and those visible in the radio band ($\nu \geq \nu_0$), p_0 is the momentum of the relativistic electrons emitting the synchrotron frequency ν_0 in a magnetic field B and $B_{cmb} = 3.25(1+z)^2$ μG accounts for inverse Compton scattering of cosmic microwave background photons.

In a DSA regime, e.g., [26], the particle injection spectrum is $Q(p) \propto p^{-\delta_{inj}}$, with slope related to the shock Mach number via

$$\delta_{inj} = 2\frac{\mathcal{M}^2 + 1}{\mathcal{M}^2 - 1}\,. \tag{5}$$

For $\mathcal{M} = 1.7 - 1.8$, Equation (5) implies $\delta_{inj} = 4 - 3.8$ (and integrated spectral index $\alpha = \delta_{inj}/2 = 2 - 1.9$). Therefore, in the case of the relic in A115, the predicted synchrotron spectral index is not consistent with its observed value $\alpha \sim 1.1$ [5] and it also would require an untenable large acceleration efficiency from Equation (3). This rules out particle acceleration from the thermal pool.

If we assume that a population of seed electrons already exists in the ICM, the initial (upstream) and accelerated spectra of electrons are connected via

$$N_d(p) = (\delta_{inj} + 2) p^{-\delta_{inj}} \int_{p_{min}}^{p} x^{\delta_{inj}-1} N_u(x)\, dx \tag{6}$$

where N_u refers to the upstream spectrum of seed particles and p_{min} is the minimum particle momentum of accelerated electrons. In Figure 3 we show the electron acceleration efficiency versus the downstream magnetic field in the case of electrons with $p_{min}/m_e c = 20$ and 200 and spectrum $Q(p) \propto p^{-3.8}$. Not all the combinations of (η_e, B) are feasible in Figure 3. In particular, even if η_e can be larger in re-acceleration than in the case of acceleration, e.g., [2], values above few per cent are still problematic, e.g., [27]. In addition, although current limits on the magnetic field in radio relics reveal strengths above a few μG, e.g., [10,28–30], the presence of $B \geq 10$ μG in cluster outskirts is unlikely and this further reduces the allowed region in the (η_e, B) plane, marked in green in Figure 3. Taking into accounts these considerations, re-acceleration of electrons with $p_{min} \geq 100\, m_e c$ appears energetically viable. Note, however, that in this case the spectrum of the relic would be very steep ($\alpha \sim 2$).

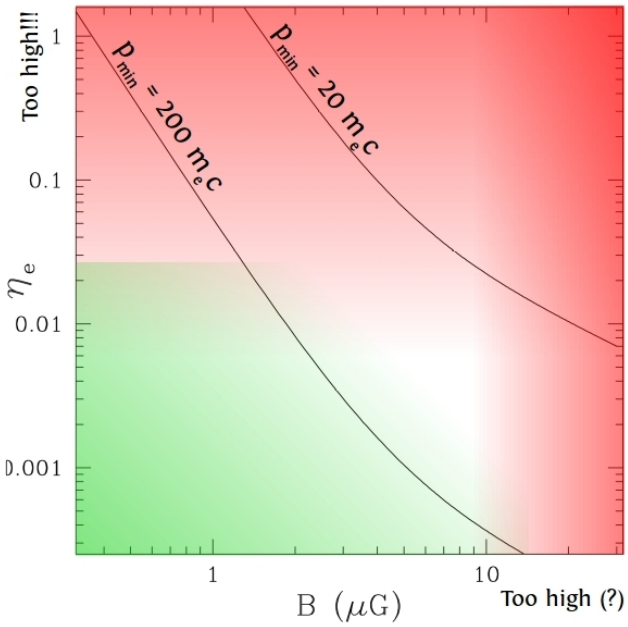

Figure 3. Electron acceleration efficiency versus magnetic field downstream in the shock in A115. Lines represent efficiencies evaluated for re-accelerated electrons with $p_{min}/m_e c = 20$ (top) and 200 (bottom) and $\delta_{inj} = 3.8$. The green region marks the allowed combinations of (B, η_e).

The spectral index problem can be coped with by assuming that the shock is re-accelerating a cloud of electrons with flatter spectrum that are not very old, boosting their emission at higher frequencies and preserving the original spectrum (Equation (6), see, e.g., [25], for details). This scenario is suggested by the presence of few radiogalaxies embedded in the relic. These could naturally provide the seed electrons and alleviate the problem of the relic E part, which lays in a region where the thermal energy density is small, hence it further stresses the DSA theory due to the larger acceleration efficiency that would be implied. In conclusion, re-acceleration models recently invoked to explain the origin of some radio relics, e.g., [13,15,31] appear a promising solution to the CRs production in weak cluster shocks. However, we mention that it is still not clear if particles non-uniformly injected in the ICM by cluster radiogalaxies are able to reproduce the observed regular morphologies of radio relics on ∼Mpc scales. For these reasons this scenario certainly deserves more investigation in the future.

4. Conclusions

A115 is a dinamically disturbed galaxy cluster located at $z = 0.197$. We presented the study of the northern outskirts of the cluster, where a giant radio relic is located. The deep *Chandra* observations (334 ks) and the re-analysis of an archival VLA dataset led to the following results:

- The discovery of a shock in the N part of the cluster. The Mach numbers derived via SB and temperature jump are consistent, leading to $\mathcal{M}_{\rm SB} = 1.7 \pm 0.1$ and $\mathcal{M}_{\rm kT} = 1.8^{+0.5}_{-0.4}$, respectively.
- The shock is co-spatially located with the W part of the radio relic. This strongly supports the idea that shocks play a crucial role in the formation of relics.
- The low Mach number of the shock in A115, compared to the spectral index of relic, rules out particle acceleration from the thermal pool. On the other hand, a scenario where the shock is re-accelerating CRs injected in the ICM by the surrounding radiogalaxies appears energetically favored.
- The E part of the relic is located in a low X-ray SB region which does not allow a clear investigation with current *Chandra* data. However, the relic morphology is consistent with numerical simulations of an off-axis merger between galaxy clusters with different mass, where the shock bends around the less massive cluster. In this respect, we propose that this relic region is due to the uplifting of the radiogalaxies plasma by the shock spreading out in the cluster outskirts.

Future radio observations aimed to study the spectral index across the relic will help to disclose the origin of the source. In particular, new instruments such as LOFAR, SKA and a number of its precursors, will enter into unexplored territories, reaching unprecedented sensitivities to cluster scale emission over a broad frequency range. These data will extend the frequency range allowing to highlight the effect due to additional mechanisms in the downstream region, such as particle re-acceleration. Deeper X-ray observations are also required to investigate the NE periphery of the cluster, where the E part of the relic stands out.

Acknowledgments: The scientific results reported in this article are based on observations made by the *Chandra* X-ray Observatory. The NRAO is a facility of the National Science Foundation operated under cooperative agreement by Associated Universities, Inc. A.B. and G.B. acknowledge partial support from PRIN-INAF 2014. F.G. acknowledges financial support from PRIN-INAF 2012 and ASI-INAF I/037/12/0.

Author Contributions: A.B. wrote this contribution. A.B. and F.G. performed the X-ray data analysis. A.B. and D.D. performed the radio data analysis. G.B. carried out the calculations on the (re)acceleration efficiency.

Conflicts of Interest: The authors declare no conflict of interest.

Abbreviations

The following abbreviations are used in this manuscript:

CR	cosmic ray
DSA	diffusive shock acceleration
ICM	intra-cluster medium
SB	surface brightness
SNR	supernova remnant
VLA	*Very Large Array*

References

1. Feretti, L.; Giovannini, G.; Govoni, F.; Murgia, M. Clusters of galaxies: observational properties of the diffuse radio emission. *Astron. Astrophys. Rev.* **2012**, *20*, 54.
2. Brunetti, G.; Jones, T. Cosmic Rays in Galaxy Clusters and Their Nonthermal Emission. *Int. J. Mod. Phys. D* **2014**, *23*, 1430007.
3. Eckert, D.; Molendi, S.; Paltani, S. The cool-core bias in X-ray galaxy cluster samples. I. Method and application to HIFLUGCS. *Astron. Astrophys.* **2011**, *526*, A79.
4. Bartalucci, I.; Mazzotta, P.; Bourdin, H.; Vikhlinin, A. Chandra ACIS-I particle background: an analytical model. *Astron. Astrophys.* **2014**, *566*, A25.
5. Govoni, F.; Feretti, L.; Giovannini, G.; Böhringer, H.; Reiprich, T.H.; Murgia, M. Radio and X-ray diffuse emission in six clusters of galaxies. *Astron. Astrophys.* **2001**, *376*, 803–819.
6. Forman, W.; Bechtold, J.; Blair, W.; Giacconi, R.; van Speybroeck, L.; Jones, C. Einstein imaging observations of clusters with a bimodal mass distribution. *Astrophys. J.* **1981**, *243*, L133–L136.
7. Shibata, R.; Honda, H.; Ishida, M.; Ohashi, T.; Yamashita, K. Temperature Variation in the Cluster of Galaxies Abell 115 Studied with ASCA. *Astrophys. J.* **1999**, *524*, 603–611.
8. Gutierrez, K.; Krawczynski, H. The Off-Axis Galaxy Cluster Merger A115. *Astrophys. J.* **2005**, *619*, 161–168.
9. Barrena, R.; Boschin, W.; Girardi, M.; Spolaor, M. The dynamical status of the galaxy cluster Abell 115. *Astron. Astrophys.* **2007**, *469*, 861–872.
10. Finoguenov, A.; Sarazin, C.; Nakazawa, K.; Wik, D.; Clarke, T. XMM-Newton Observation of the Northwest Radio Relic Region in A3667. *Astrophys. J.* **2010**, *715*, 1143–1151.
11. Akamatsu, H.; Kawahara, H. Systematic X-Ray Analysis of Radio Relic Clusters with Suzaku. *Publ. Astron. Soc. Jpn.* **2013**, *65*, 16.
12. Bourdin, H.; Mazzotta, P.; Markevitch, M.; Giacintucci, S.; Brunetti, G. Shock Heating of the Merging Galaxy Cluster A521. *Astrophys. J.* **2013**, *764*, 82.
13. Shimwell, T.; Markevitch, M.; Brown, S.; Feretti, L.; Gaensler, B.; Johnston-Hollitt, M.; Lage, C.; Srinivasan, R. Another shock for the Bullet cluster, and the source of seed electrons for radio relics. *Mon. Not. R. Astron. Soc.* **2015**, *449*, 1486–1494.

14. Eckert, D.; Jauzac, M.; Vazza, F.; Owers, M.; Kneib, J.P.; Tchernin, C.; Intema, H.; Knowles, K. A shock front at the radio relic of Abell 2744. *Mon. Not. R. Astron. Soc.* **2016**, *461*, 1302–1307.
15. Botteon, A.; Gastaldello, F.; Brunetti, G.; Dallacasa, D. A shock at the radio relic position in Abell 115. *Mon. Not. R. Astron. Soc.* **2016**, *460*, L84–L88.
16. Botteon, A.; Gastaldello, F.; Brunetti, G.; Kale, R. A $\mathcal{M} \gtrsim 3$ shock in 'El Gordo' cluster and the origin of the radio relic. *Mon. Not. R. Astron. Soc.* **2016**, *463*, 1534–1542.
17. Van Weeren, R.; Brüggen, M.; Röttgering, H.; Hoeft, M. Using double radio relics to constrain galaxy cluster mergers: a model of double radio relics in CIZA J2242.8+5301. *Mon. Not. R. Astron. Soc.* **2011**, *418*, 230–243.
18. Ricker, P.; Sarazin, C. Off-Axis Cluster Mergers: Effects of a Strongly Peaked Dark Matter Profile. *Astrophys. J.* **2001**, *561*, 621–644.
19. Vazza, F.; Brüggen, M. Do radio relics challenge diffusive shock acceleration? *Mon. Not. R. Astron. Soc.* **2014**, *437*, 2291–2296.
20. Vazza, F.; Eckert, D.; Brüggen, M.; Huber, B. Electron and proton acceleration efficiency by merger shocks in galaxy clusters. *Mon. Not. R. Astron. Soc.* **2015**, *451*, 2198–2211.
21. Vazza, F.; Brüggen, M.; Wittor, D.; Gheller, C.; Eckert, D.; Stubbe, M. Constraining the efficiency of cosmic ray acceleration by cluster shocks. *Mon. Not. R. Astron. Soc.* **2016**, *459*, 70–83.
22. Markevitch, M.; Govoni, F.; Brunetti, G.; Jerius, D. Bow Shock and Radio Halo in the Merging Cluster A520. *Astrophys. J.* **2005**, *627*, 733–738.
23. Kang, H.; Ryu, D.; Jones, T. Diffusive Shock Acceleration Simulations of Radio Relics. *Astrophys. J.* **2012**, *756*, 97.
24. Pinzke, A.; Oh, S.; Pfrommer, C. Giant radio relics in galaxy clusters: reacceleration of fossil relativistic electrons? *Mon. Not. R. Astron. Soc.* **2013**, *435*, 1061–1082.
25. Kang, H.; Ryu, D. Re-acceleration Model for Radio Relics with Spectral Curvature. *Astrophys. J.* **2016**, *823*, 13.
26. Blandford, R.; Eichler, D. Particle acceleration at astrophysical shocks: A theory of cosmic ray origin. *Phys. Rep.* **1987**, *154*, 1–75.
27. Kang, H.; Ryu, D. Re-acceleration of Non-thermal Particles at Weak Cosmological Shock Waves. *Astrophys. J.* **2011**, *734*, 18.
28. Bonafede, A.; Giovannini, G.; Feretti, L.; Govoni, F.; Murgia, M. Double relics in Abell 2345 and Abell 1240. Spectral index and polarization analysis. *Astron. Astrophys.* **2009**, *494*, 429–442.
29. Van Weeren, R.; Röttgering, H.; Brüggen, M.; Hoeft, M. Particle Acceleration on Megaparsec Scales in a Merging Galaxy Cluster. *Science* **2010**, *330*, 347.
30. Botteon, A.; Brunetti, G.; Dallacasa, D. Constraining magnetic field strength in radio relics. In Proceedings of the Many Facets of Extragalactic Radio Surveys: Towards New Scientific Challenges, Bologna, Italy, 20–23 October 2015; p. 46.
31. Bonafede, A.; Intema, H.; Brüggen, M.; Girardi, M.; Nonino, M.; Kantharia, N.; van Weeren, R.; Röttgering, H. Evidence for Particle Re-acceleration in the Radio Relic in the Galaxy Cluster PLCKG287.0+32.9. *Astrophys. J.* **2014**, *785*, 1.